Summary: We report the synthesis of star-shaped poly(acrylic acid) (PAA), with 5, 8, and 21 arms, by atom transfer radical polymerization of *tert*-butyl acrylate. We employ the core-first approach using glucose-, saccharose- and cyclodextrin-based initiators. Subsequent acidic treatment of poly(*tert*-butyl acrylate) (PtBA) leads to star-shaped poly(acrylic acid) (PAA). Alkaline cleavage of the arms enabled us to determine the initiation site efficiency. The PAA stars and arms were esterified to poly(methyl acrylate) (PMA). Molecular weight determination by means of GPC/viscosity, MALDI-TOF MS and NMR end-group determination showed that the initiation site efficiency is close to unity. Results from potentiometric titration of PAA arms and stars show that the apparent pK_a values increase with increasing arm number, which is a direct result of increasing segment density. Osmometry measurements of aqueous solutions of the PAA stars result in osmotic coefficients between 0.05 and 0.38, indicating that most of the counterions are confined within the star. The confinement increases with arm number.

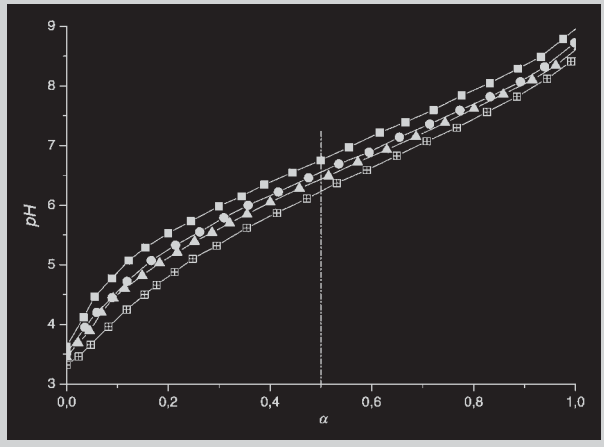

Potentiometric titration curves for stars $(PAA_{100})_{21}$, $(PAA_{100})_8$, $(PAA_{100})_5$, and linear PAA_{100}.

Synthesis, Characterization and Behavior in Aqueous Solution of Star-Shaped Poly(acrylic acid)

Felix A. Plamper,[1] *Harald Becker,*[1] *Michael Lanzendörfer,*[1a] *Mushtaq Patel,*[2] *Alexander Wittemann,*[2] *Matthias Ballauff,*[2] *Axel H. E. Müller**[1]

[1] Makromolekulare Chemie II, Bayreuther Zentrum für Kolloide und Grenzflächen, Universität Bayreuth, D-95440 Bayreuth, Germany
Fax: +49-921-553393; E-mail: axel.mueller@uni-bayreuth.de
[2] Physikalische Chemie I, Bayreuther Zentrum für Kolloide und Grenzflächen, Universität Bayreuth, D-95440 Bayreuth, Germany

Received: June 7, 2005; Revised: July 19, 2005; Accepted: July 20, 2005; DOI: 10.1002/macp.200500238

Keywords: atom transfer radical polymerization (ATRP); osmotic coefficient; polyelectrolytes; polymer synthesis; potentiometric titration; star polymers

Introduction

Polyelectrolytes with non-linear topologies have attracted considerable interest in recent years. Rod-like polyelectrolytes[1,2] have proven to be a good model for the experimental verification of Fuoss',[3] Osawa's[4] and Manning's[5] predictions about the counterion condensation: the reduction of osmotically active counterions due to electrostatic attraction to the highly charged polyelectrolyte backbone. The situation is more complicated for branched polyelectrolytes with hyperbranched,[6,7] star-, comb-, or brush-like structures.[8,9] Planar,[9,10] spherical[11] and cylindrical[12,13] polyelectrolyte brushes have been prepared. The swelling behaviour of spherical brushes, which depends on the pH,[14] the ionic strength[14] and the counterions,[15] was investigated. The osmotic coefficient ϕ, which is a measure of counterion condensation, is defined as the ratio of the measured osmotic pressure and the theoretical osmotic pressure, according to van't Hoff's law.[16] The osmotic coefficient of spherical brushes[17] has been seen to be reduced by one order of magnitude compared to linear polyelectrolytes.[18–21] Intermediate effects on counterion condensation are expected for star-shaped polyelectrolytes, as predicted by previous work.[22] Scaling theory, together with self-consistent field calculations of polyelectrolyte stars, were given by Klein Wolterink et al.[23,24] and Borisov and Zhulina.[25,26] Ordered, crystalline phases are expected at higher concentrations and arm numbers.[27,28] The first

[a] Deceased.

experimental proof of such phases was given by Furukawa and Ishizu.[29]

Potentiometric titrations of linear polyacids and polybases have been performed and discussed.[18,30–32] In contrast to low molecular acids, where distinct deprotonation equilibrium constants, due to distinct ionization processes, can be observed, for polyacids only average equilibrium constants depending on ionization degree can be extracted. A polymer's architecture changes its titration behavior,[24,33] as was shown for hyperbranched polyacids[6] and predicted by Klein Wolterink et al.[24] for star-shaped weak polyacids by self-consistent field calculations.

Star-shaped polyelectrolytes have been synthesized by different approaches. The arm-first strategy was used by Mays et al., linking polystyryl lithium arms with divinylbenzene, followed by sulfonation to yield poly(styrene sulfonate) stars.[34,35] Similarly, living anionic poly(*tert*-butyl acrylate) (PtBA) arms were coupled by ethylene glycol dimethacrylate,[36] followed by elimination of isobutylene to form poly(acrylic acid) (PAA) stars.[8] Later, the same attempt was taken up using atom transfer radical polymerization (ATRP).[29] The arm-first method with difunctional monomers leads to large numbers of arms, but with a rather broad distribution of arm number. In contrast, defined multifunctional terminating agents circumvent this problem. Thus, poly(methacrylic acid) (PMAA) and PAA stars with three, four, and eight arms[37,38] were obtained.

In the core-first approach polymerization is conducted from an oligofunctional initiator, leading to well-defined stars with a precisely defined arm number. This approach was applied to the synthesis of PAA stars using ATRP of tBA. Schnitter et al.[39] used an initiator with six α-bromoester functions, esterified with a dendritic core, whereas Moinard et al.[40] used a core carrying four benzyl bromide functions.

In this paper we describe the synthesis and characterization of star-shaped poly(acrylic acid) with five, eight, and 21 arms. In contrast to Schnitter's core-first attempt[39] we attached 2-bromoisobutyrate initiator functions to sugars, namely α-D-glucose, saccharose and β-cyclodextrin.[41–44] ATRP of tBA leads to the corresponding poly(*tert*-butyl acrylate) stars. These were transformed to poly(acrylic acid) stars by acidic isobutylene elimination. The PAA stars were used to investigate the aqueous solution behavior of star-shaped, weak polyelectrolytes, in particular, counterion condensation by means of osmometry. For this purpose, potentiometric titrations were also performed.

This paper is organized as follows: Firstly, we describe the synthesis of PAA stars and the molecular characterization of both stars and single arms. Then we show potentiometric titrations and osmometry performed on these stars. Those measurements show that star-shaped PAA differs significantly from its linear analogue. A detailed discussion of those effects will be given in a separate paper.

Experimental Part

Materials

2-Bromoisobutyryl bromide, *N*,*N*,*N*′,*N*′,*N*″-pentamethyldiethylenetriamine (PMDETA), CuBr, 4-(*N*,*N*-dimethylamino)-pyridine, CF_3COOH, 1,4-dioxane, *trans*-3-indolacrylic acid (IAA), 2,5-dihydroxybenzoic acid (DHB), trimethylsilyldiazomethane and acidic ion-exchange resin (Dowex Marathon) were purchased from Aldrich. α-D-Glucose, pyridine, CH_2Cl_2, tetrahydrofuran (THF), silica gel 60, methanol (MeOH) and $CHCl_3$ were purchased from Merck. Saccharose was purchased from Aldi-Süd, and β-cyclodextrin was supplied by Avocado, Heysham, UK. These chemicals were taken as delivered (except PMDETA, which was distilled and degassed, and CuBr, which was treated with pure acetic acid and filtered to remove traces of Cu(II) compounds). *tert*-Butyl acrylate was donated by BASF. It was distilled, and the first and last fractions were discarded, to remove low molecular mass inhibitor. Irganox 1010 stabilizer (Ciba) was added before the monomer was condensed on the vacuum line to finally degas it, with the help of three freeze-thaw cycles. Chemicals needed for polymerization were transferred into the glove box.

Synthesis of Oligo-Initiators

A typical preparation procedure is described for heptakis[2,3,6-tri-*O*-(2-bromoisobutyryl)]-β-cyclodextrin:[41,42] β-Cyclodextrin (21.4 g; 0.019 mol) was dehydrated in a vacuum oven at 80 °C for 1 h. It was then suspended in 120 mL pyridine and 250 mL chloroform. One tip of a spatula of 4-(*N*,*N*-dimethylamino)pyridine was added as a catalyst, before the mixture was cooled with ice. By use of a dropping funnel, 2-bromoisobutyryl bromide (184 g; 0.8 mol) was added within 4 h to the suspension. The mixture was stirred for one day at room temperature and then refluxed for 3 h. The pyridinium bromide was removed by filtration. The liquid was carefully washed twice with 1 N HCl, once with concentrated $NaHCO_3$ solution, once with 1 N NaCl solution and finally with water. The organic phase was dried with Na_2SO_4 and concentrated using a rotational evaporator. The yellow-brownish residue was chromatographed over a silica column (toluene:ethyl acetate = 3:1 by vol.) which resulted a yellow solid (28.3 g; 35% yield). The product was further purified to an almost colorless solid by recrystallization from warm hexane (15.17 g; 19% yield). Full esterification was confirmed by MALDI-TOF mass spectrometry (matrix DHB; mass ratio DHB:LiCl:initiator 10:1:1; reflection mode and linear mode; $M(+Li^+) = 4\,267\ g \cdot mol^{-1}$). ^1H NMR ($CDCl_3$): $\delta = 1.8$ (broad s, 126H, CH_3), 3.5–5.4 (49 H, sugar protons).

Analogous procedures were used for the preparation of 2,3,4,6,1′,3′,4′,6′-octa-*O*-(2-bromoisobutyryl)saccharose and 1,2,3,4,6-penta-*O*-(2-bromoisobutyryl)-α-D-glucose using saccharose or α-D-glucose as a scaffold.[42–44] The workup changed so far as pyridinium bromide was not filtered, but rather removed by repeated extraction with cold water after the mixture was diluted with ≈100 mL of diethyl ether. The organic phase was concentrated, after it was extracted with concentrated $NaHCO_3$ solution. The solid was washed with cold methanol. Drying in a vacuum oven yielded a white

powder (yield: 73% for the glucose-based initiator and 72% for the saccharose-based initiator). Saccharose-based initiator: $M(+Li^+) = 1\,541\ g \cdot mol^{-1}$ by MALDI-TOF MS (DHB: LiCl:initiator 10:1:1). Glucose-based initiator: $M(+Li^+) = 931\ g \cdot mol^{-1}$.

Synthesis of Poly(tert-butyl acrylate) Stars

A typical polymerization procedure proceeds as follows:[39] In a glove box, CuBr (14.6 mg; 0.102 mmol) and initiator (e.g. cyclodextrin-based initiator: 50 mg; 1.17×10^{-5} mol) were weighed and placed in a 50 mL round bottom flask which was tightly closed with a seal bearing a septum. *tert*-Butyl acrylate (tBA) (10.4 g; 81 mmol) and ligand PMDETA (21.3 mg; 0.123 mmol) were added. The molar ratio [initiation site]:[PMDETA]:[CuBr] was about 1:0.50:0.42 and should be readjusted when aiming for different arm lengths. The initially heterogeneous mixture was stirred outside the glove box at 60 °C to 65 °C in an oil bath. The monomer conversion, x_p, was traced by taking samples through the septum under nitrogen counter flow, and comparing the NMR signals of the monomer (vinylic protons at 6.3 ppm) and the polymer (methine protons at 2.2 ppm). The conversion was used to calculate the theoretical degree of polymerization (DP) per arm:

$$DP_{n,\mathrm{theo,arm}} = x_p \times [\mathrm{tBA}]_0/[\mathrm{inisite}]_0 \quad (1)$$

where $[\mathrm{tBA}]_0$ and $[\mathrm{inisite}]_0$ are the initial monomer and initiation site concentrations, respectively. After 9 h the monomer conversion was 38.4% and the reaction was stopped by diluting the yellow-green, viscous mixture with acetone (or THF) in presence of oxygen. The solution was then filtered over silica gel to remove any copper compounds. The obtained poly(*tert*-butyl acrylate) (PtBA) was freeze-dried from dioxane, which yields 3.1 g polymer after drying in vacuum oven at 40 °C. The different experimental conditions for the synthesis of the different PtBA star polymers are shown in Table 1.

Transformation to Poly(acrylic acid)[6,13]

PtBA (2.3 g) was dissolved in about 20 mL of dichloromethane, which results in a slightly yellow solution. After addition of trifluoroacetic acid (10.5 g) the color of the mixture turned darker, and, after one night with stirring at room temperature, the PAA had precipitated. The white precipitate was dissolved in 20 mL dioxane and 4 mL methanol and freeze-dried to remove trifluoroacetic acid, which gave 1.3 g of PAA star.

Cleavage of Arms by Alkaline Hydrolysis

0.1 g of PAA stars and about 0.2 g NaOH were dissolved in approximately 2 mL of water (in polyethylene vials) and heated for 5 days at 80 °C. The pure linear PAA was then recovered by use of a sufficient amount (≈5 g) of acidic ion exchange resin until reaching pH ≈ 3. The resin was removed and the aqueous solution was freeze-dried. Full cleavage was proven by comparison of the elution volumes of the star-shaped and linear PAA by means of aqueous GPC.

Methylation of PAA[45]

Star-shaped and linear PAA were methylated with trimethylsilyldiazomethane. Typically, a solution of 0.1 g of PAA in about 1 mL of water and 3 mL of THF was prepared. Then, roughly 1 mL of trimethylsilyldiazomethane (2 M in diethyl ether) was added drop-wise under vigorous stirring. When the mixture became cloudy during methylation, additional THF was added. The addition was stopped when the yellow color did not vanish within, typically, 1 h. The solvent was slowly evaporated. The crude mixture was then dissolved in a small amount of acetone and the polymer was precipitated into cold methanol (−30 °C). The viscous polymer was finally freeze-dried from dioxane. ^{1}H NMR ($CDCl_3$): $\delta = 1.4$ (s, t-butyl if present), 1.5–2.0 (methylene protons from backbone), 2.1–2.5 (methine protons), 3.32 (s, $\mathbf{CH_3}$–O–CH_2CO), 3.35–3.45 (not assigned), 3.64 (s, $\mathbf{CH_3}$–OCO), 3.9–4.2 (s, CH_3–O–$\mathbf{CH_2}$CO). ^{13}C NMR ($CDCl_3$): $\delta = 25.7$, 26.4, 28.3 ($\mathbf{C}H_3$–C, residual *tert*-butyl, initiator?), 35.4 ($\mathbf{C}H_2$–backbone), 41.7 (methine carbons), 52.1 ($\mathbf{C}H_3$–OCO), 58.9 ($\mathbf{C}H_3$–O–CH_2–CO), 64.4 ((CH_3)$_3\mathbf{C}$–O), 72.4 (CH_3–O–$\mathbf{C}H_2$–CO), 174.8, 175.2 (both carbonyl).

Purification

Purification of PAA by Dialysis

1 g of $(PAA_n)_x$ was dissolved in about 25 mL of water and dialyzed against Millipore water for typically 5 days

Table 1. Experimental conditions for the synthesis of PtBA stars, with T ≈ 65 °C, and [PMDETA]/[CuBr] ≈ 1.

Star	$[\mathrm{tBA}]_0$[a]	$[\mathrm{Inisite}]_0$	[CuBr]	t	Conversion, x_p[b]
	$mol \cdot L^{-1}$	$mmol \cdot L^{-1}$	$mmol \cdot L^{-1}$	min	
$(PtBA_{90})_5$	5.4	35	35	145	0.56
$(PtBA_{75})_8$	6.8 (bulk)	34	10	270	0.37
$(PtBA_{100})_8$	5.4	30	30	125	0.56
$(PtBA_{160})_8$	bulk	21	21	180	0.48
$(PtBA_{60})_{21}$	bulk	24	7	140	0.22
$(PtBA_{100})_{21}$	5.4	29	29	285	0.53
$(PtBA_{125})_{21}$	bulk	21	9	540	0.38

[a] The solvent for $(PtBA_{100})_8$ and $(PtBA_{100})_{21}$ was ethyl acetate.
[b] Conversion was measured by NMR spectroscopy.

(spectrapore cellulose ester membrane, MWCO 6 kDa). The purified aqueous solution was freeze-dried and then dried in a vacuum oven at 40 °C.

Purification of PAA by Ultrafiltration

15 g of $(PAA)_x$ were dissolved in 300 mL water. These solutions were ultrafiltrated (polyethersulfone membrane MWCO 10 and 30 kDa; Millipore) with approximately 10 L Millipore™ water. To prevent any potential harm to the stars like cleavage, the process was interrupted after about 3 days. The purified aqueous solution was finally freeze-dried and then dried in vacuum oven at 40 °C.

Purification of the Sodium Salt of PAA by Dialysis

Dialysis against Millipore™ water was used as the purification method to prevent germs and dust being concentrated within the sample solution. About 200 mg of PAA stars and 70 mg of NaOH were dissolved in 30 mL of Millipore™ water and filled into dialysis tubes (Spectra Pore™; regenerated cellulose membrane; $\varnothing \approx 2$ cm; MWCO: 6–8 kDa). The tubes were kept in 5 L of stirred Millipore™ water. The water was exchanged almost daily. After two weeks the purification process was stopped and the solid contents of the resulting mother solutions were determined by freeze-drying. Measurement of the pH of a 0.7 $g \cdot L^{-1}$ solution was used to determine the degree of neutralization (see Potentiometric Titration).

To verify stability of all stars during purification, we performed GPC in aqueous buffer solution of samples before and after purification.

Polymer Characterization

^1H and ^{13}C NMR Spectroscopy

A Bruker Avance (250 MHz) spectrometer was used. The concentrations in solutions were around 10 $mg \cdot mL^{-1}$ each, while the solvent was either D_2O or $CDCl_3$. Simulations were performed with ACD/HNMR and ACD/CNMR Predictor Ver.3.00.

FT-IR Spectroscopy

FT-IR spectroscopy was performed using a Bruker Equinox 55/S. Poly(methyl acrylate) (PMA) and poly(acrylic acid) (PAA) were dissolved in acetone and methanol respectively and applied to a KBr plate and dried at 80 °C for several minutes.

MALDI-TOF Mass Spectrometry

MALDI-TOF mass spectrometry was performed on a Bruker Daltonics Reflex 3 with an N_2 laser (337 nm) with a 20 kV acceleration voltage. We used trans-3-indolacrylic acid (IAA) as the matrix (mass ratio IAA:polymer = 10:1) to determine the molecular weight of PtBA and PMA polymers. Most measurements were performed in linear mode, except for polymers with number average molecular weight, $\overline{M}_n < 10\,000$ $g \cdot mol^{-1}$, where the reflection mode was used. In the case of detection of doubly charged species, a double Gaussian fit was used to extract $\overline{M}_n$ and the polydispersity index, *PDI*, of the desired species. Overlap with signals of the matrix or low molecular compounds was resolved, if necessary, by applying a Gaussian fit to the undisturbed region. Assuming the initiation efficiency, f_i, was close to unity, the stars' $\overline{M}_n$ were taken to determine $DP_{n,arm}$ by dividing $\overline{M}_n$ by the molecular weight of the repeating unit M_r and the initiation sites per initiator molecule. For PMA stars M_r was taken to be 90 $g \cdot mol^{-1}$ to reflect the residual *tert*-butyl groups and methylene insertion into the methyl ester moieties, according to the NMR spectra shown later for the methylated PAA stars in $CDCl_3$. The molecular mass of the initiator core was taken into account for the stars. For linear PMA only double methylation and the residual initiation moiety was taken into account ($M_r = 88$ $g \cdot mol^{-1}$). For simulation of the mass distribution of single molecules due to isotopic statistics we used Bruker Xtof 5.1.1 software.

Gel Permeation Chromatography (GPC)

Molecular weight distributions and averages were characterized by conventional GPC and GPC/viscosity using THF as the eluent, at a flow rate of 1.0 $mL \cdot min^{-1}$, at room temperature. A conventional THF-phase GPC system was used to obtain the apparent molecular weights. GPC system I: column set: 5 μm PSS SDV gel, 10^2, 10^3, 10^4, 10^5 Å, 30 cm each; injection volume 20 μL of a 2 $mg \cdot mL^{-1}$ solution; detectors: Waters 410 differential refractometer and Waters photodiode array detector. Narrow PS standards (PSS, Mainz) were used for the calibration of column set I. The molecular weights of the star-shaped polymers were determined by the universal calibration principle[46] using the viscosity module of the PSS WinGPC scientific V 6.1 software package on GPC system II. Linear PMMA standards (PSS, Mainz) were used to construct the universal calibration curve. GPC system II: column set: 5 μm PSS SDV gel, 10^3 Å, 10^5 Å and 10^6 Å, 30 cm each; detectors: Shodex RI-71 refractive index detector, Jasco Uvidec-100-III UV detector ($\lambda = 254$ nm), Viscotek viscosity detector H 502B, which needed to be purged extensively before every measurement. The extracted number average molecular mass $\overline{M}_n$ was used to determine the degree of polymerization $DP_{n,arm}$ of one arm by dividing $\overline{M}_n$ by the molar mass of the polymer's repeating unit and, for stars, by the initiation sites per initiator molecule (assuming $f_i = 1$). The initiator was taken into account. The third setup was an aqueous GPC (internal standard ethylene glycol; additives: 0.1 M NaN_3, 0.01 M NaH_2PO_4), which validated that the PAA stars were intact both before and after the purification steps. Column set: two 8 mm PL Aquagel-OH columns (mixed and 30 Å), operated at 35 °C. Detector: Bischoff RI-Detector 8110.

Potentiometric Titration

In order to determine the degree of neutralization at ambient temperatures we carried out potentiometric titrations of PAA stars at crude mass concentrations of 0.6 $g \cdot L^{-1}$ ($(PAA_{75})_8$ and $(PAA_{160})_8$) to 0.7 $g \cdot L^{-1}$ (for all other stars), which is within the concentration range of our osmotic pressure measurements. Adsorbed water and residual *tert*-butyl can reduce the molar carboxyl concentration by up to 20% ([COOH] ≈ 8 $mmol \cdot L^{-1}$]). To complete the series, we also titrated linear

PAA, which was cleaved from $(PAA_{100})_{21}$. We used a CG 840 (Schott) pH meter, which was calibrated by buffer solutions. The titration was carried out with 0.048 N NaOH, such that the volume change does not exceed 20%. One titration took about one hour. The equivalence point of the titration is set as the point of intersection of the inflection tangents of the titration curve at high pH. The steep increase in pH at the end of titration is caused by excess NaOH. The equivalence point, which is theoretically determined by knowledge of the added masses, is imprecise, as it is difficult to obtain PAA, which is totally water free. When measuring titration curves on different days, a system that had been previously measured was again investigated as a comparison, such that the whole new data set could be shifted to the old values, to obtain relative correctness. The shift in pH (due to changes in temperature and calibration solutions) of the same system at different times is small, being within 0.08 pH units.

Osmometry

A Gonotec Osmomat 090 membrane osmometer was used for the determination of the osmotic coefficient. The cell was kept at 30 °C. We used a Sartorius cellulose triacetate membrane (nominal molecular weight cut-off of 5 kDa). Directly after purification of the partially neutralized PAA stars, the mother solutions obtained were used to prepare a concentration series by dilution with Millipore water. To rinse the measurement cell with a new sample, 1 mL of sample solution was injected about five times. In the case of purified salts of $(PAA_n)_x$ the osmotic pressure is constant after the rise due to injection. Therefore no rinsing with pure water is necessary between injections of different samples. The osmotic pressure was taken to determine the osmotic coefficient.

Results and Discussion

Synthesis and Characterization of Oligo-Initiators

The ATRP oligo-initiators based on α-glucose and saccharose (1,2,3,4,6-penta-*O*-(2-bromoisobutyryl)- α-glucose and 2,3,4,6,1′,3′,4′,6′-octa-*O*-(2-bromoisobutyryl)saccharose) were synthesized similarly to procedures described by Haddleton et al.[41,43,44] and modified by Stenzel-Rosenbaum et al.[42] The synthesis of the initiator based on *β*-cyclodextrin (heptakis[2,3,6-tri-*O*-(2-bromoisobutyryl)]- *β*-cyclodextrin;[41] Scheme 1) was conducted according to the synthesis based on α-cyclodextrin.[41,42]

As shown in Figure 1, full esterification could be proven by MALDI-TOF mass spectrometry ($M(+Li^+) = 4\,267$ g · mol^{-1}, $C_{126}H_{175}O_{56}Br_{21}Li^+$). The MALDI-TOF spectra also show a series of peaks attributed to HBr elimination during the ionization process. In reflector mode an additional superposition of badly resolved peaks is observed. These are not seen in linear mode (see inset "e" in Figure 1). Thus, it is very likely that in linear mode we see fragments, which are developed during flight, and detected simultaneously with the originating ions. The reflector cannot however refocus incoming fragments with the same velocity but different masses. This results in a shift in the peak location. This confirms our assumption of consecutive HBr elimination during the MALDI ionization procedure.

The poorly resolved peak at 4 340 g · mol^{-1} may either originate from an HBr adduct of $M(+Li^+)$ ($C_{126}H_{176}O_{56}Br_{22}Li^+$) or give evidence of the open structure depicted on the right-hand side of Scheme 1 after single HBr

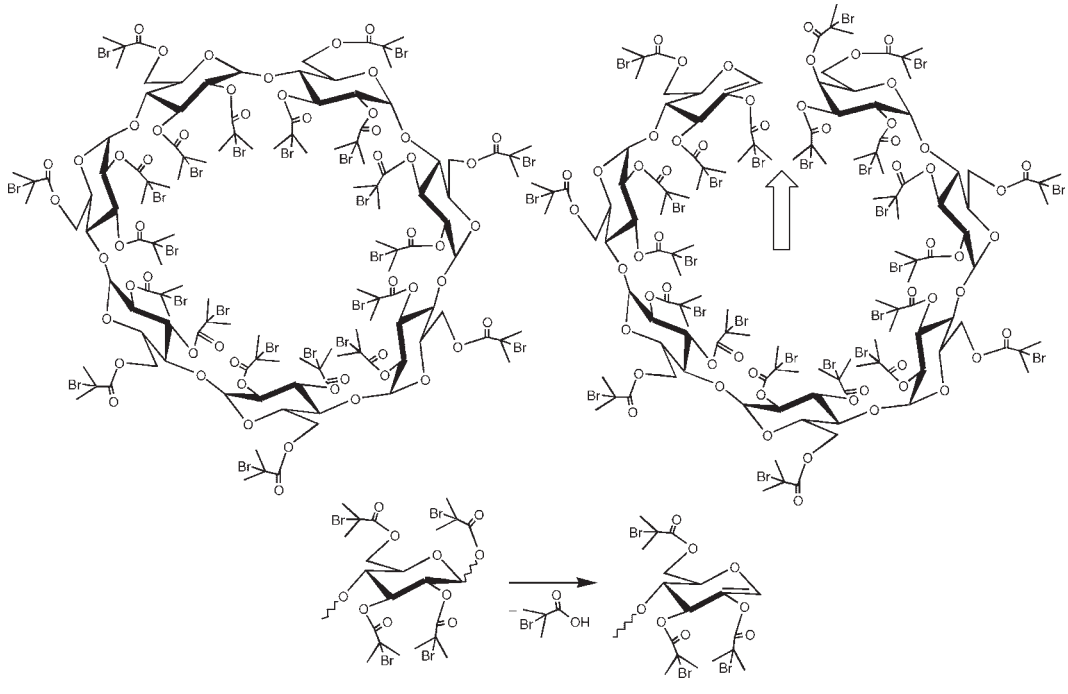

Scheme 1. Left: Full 2-bromoisobutyryl ester of *β*-cyclodextrin; right: possible species assigned to signal in MALDI-TOF MS spectra; bottom: possible pathway to the formation of the detected species.

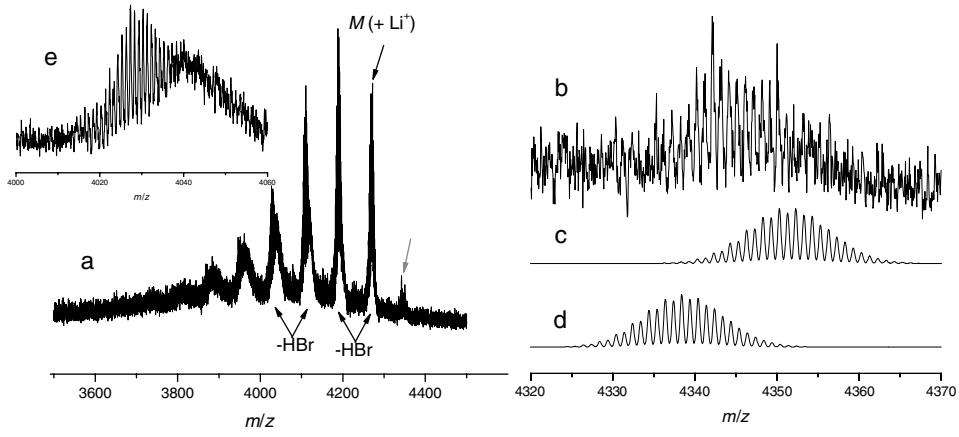

Figure 1. **a**: MALDI-TOF-MS of cyclodextrin-based ATRP oligo-initiator (reflector mode); the peak at $m/z = 4\,340$ is assigned to HBr adduct or possible side product (see Scheme 1); **b**: cut-out of peak at m/z 4 340, and comparison with simulated spectrum of side product (d) and with simulated spectrum of HBr adduct (c); **e**: cutout of spectrum at 4 030 g · mol^{-1}; matrix DHB, LiCl.

elimination ($C_{130}H_{179}O_{57}Br_{21}Li^+$). Comparison of the measured and simulated spectra in Figure 1 suggests both possibilities may contribute. The open structure formation can be assumed due to a ring opening of the β-cyclodextrin scaffold, either leading directly to an unsaturated species, or leading to a saturated glucose terminus. The anomeric hydroxyl group could then have been esterified as well (initiator with 23 initiation sites; structure on the bottom left in Scheme 1), followed by elimination of a whole ester moiety (reaction in Scheme 1). The latter can be explained by the outstanding reactivity of the ester group attached to the anomeric C atom, which easily enables elimination, especially under MALDI-TOF conditions.

MALDI-TOF MS was also performed with the glucose- and saccharose-based initiators (Figure 2). In the case of the saccharose-based initiator we could detect a small fraction of initiator with only seven initiation sites (13 mol-%), whereas the glucose was fully esterified. In both cases HBr eliminations occur, but in addition we find peaks corresponding to HBr adducts.

Synthesis and Characterization of Poly(acrylic acid) Stars

The procedure for the synthesis and complete analysis of the PAA stars consists of the following steps:

1. synthesis of PtBA stars and determination of total $\overline{M}_n$ by GPC/viscosity measurements,
2. transformation of the PtBA stars to star-shaped PAA and analysis using ^{1}H NMR spectroscopy and aqueous GPC,
3. alkaline cleavage of the PAA arms from the initiator core and analysis by ^{1}H NMR spectroscopy and aqueous GPC,
4. re-esterification of the PAA stars and cleaved-off PAA arms to poly(methyl acrylate) (PMA) and analysis by ^{1}H and ^{13}C NMR spectroscopy, and MALDI-TOF MS.

The synthesis of star-shaped poly(*tert*-butyl acrylate), $(PtBA_n)_x$ (x equals arm number, n equals degree of polymerization of arms, $DP_{n,arm}$), by ATRP was conducted analogously to the procedure by Schnitter et al.,[39] who used dendritic initiators. For this study we prepared samples with 21, 8 and 5 arms and differing arm lengths by use of the sugar-based initiators described above. The arm lengths and initiation site efficiencies were determined by means of molecular weight determinations. The typical key steps of characterization will be explained in the following for stars with 21 arms. For the stars with different arm numbers the characterization was conducted analogously. All results of the molecular weight determinations and the comparison with the expected values are summarized in Table 2.

Absolute molecular weights were determined by GPC with viscosity detection (Figure 3). The $(PtBA_n)_x$ stars always showed a discrimination of higher molecular weights in MALDI-TOF MS, thus no reliable MS data could be obtained. We believe that this is due to elimination of isobutylene during the ionization/desorption process. Even for low molecular weight PtBA standards, single species could not be resolved and no sequence of elimination processes could be detected in reflectron mode. This can also be explained by considerable decomposition during the MALDI process.

Elimination of isobutylene catalyzed by trifluoroacetic acid resulted in poly(acrylic acid) stars, which were assigned as $(PAA_n)_x$. According to ^{1}H NMR spectroscopy, elimination yields were $\geq$95% in all cases (see Figure 4). Aqueous GPC revealed that the vast majority of arms remain attached to the core during elimination, as the

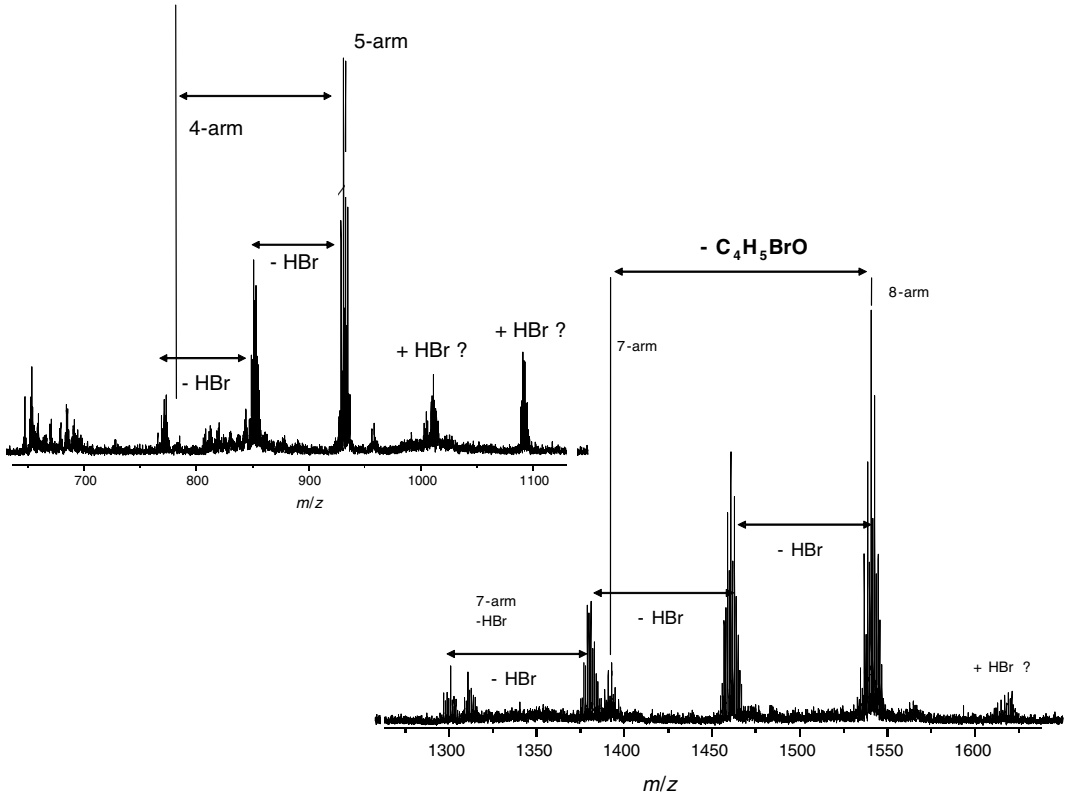

Figure 2. MALDI-TOF MS reflectron mode spectra of saccharose-based initiator (right) and glucose-based initiator (left); matrix DHB, LiCl.

amount of linear polymer was found to be $\leq$5 wt.-% (see Figure 5).

In order to determine the lengths of the arms of the $(PAA_n)_x$ stars, the arms were cleaved off the core by alkaline hydrolysis. The resulting linear PAA shows ^{1}H NMR signals from the methyl protons of the isobutyric acid initiator moiety ($\delta = 1.1$ ppm), which were not seen in the PAA star due to the low mobility of the segments near the core (Figure 4). They appear as a pseudo-doublet due to their vicinity to the chiral C atom in the first monomer unit of the polymer. Almost full cleavage was obtained using a four-fold excess of NaOH, compared to carboxylic groups. Cleavage was again verified by aqueous GPC (see Figure 5), whereas NMR spectroscopy showed that also the residual

Table 2. Number-average degrees of polymerization of the arms in the poly(acrylic acid) stars $(PAA_n)_x$ and polydispersity indices (in brackets) of respective stars and arms measured by different methods and the efficiencies of the initiation sites derived therefrom.

	Expected[a]	GPC (linear PS calibration) of PtBA stars[b]	GPC of PtBA stars using universal calibration[b]	MALDI-TOF of PMA stars[b]	MALDI-TOF of PMA arms				NMR of PAA arms			
	DP	DP, PDI	DP, PDI	DP, PDI	DP, PDI	$f_{i,conversion}$[c]	$f_{i,Univ.cal}$[d]	$f_{i,MALDI}$[e]	DP	$f_{i,conversion}$[c]	$f_{i,Univ.cal}$[d]	$f_{i,MALDI}$[e]
$(PAA_{90})_5$	86	70 (1.05)	–	100 (1.04)	107 (1.13)	0.80	–	0.93	83	1.04	–	1.20
$(PAA_{75})_8$	73	60 (1.08)	76 (1.18)	65 (1.04)	88 (1.32)	0.83	0.86	0.74	67	1.09	1.13	0.97
$(PAA_{100})_8$	101	64 (1.06)	–	114 (1.05)	130 (1.20)	0.78	–	0.88	120	0.84	–	0.95
$(PAA_{160})_8$	155	94 (1.09)	160 (1.12)	153 (1.06)	186 (1.28)	0.83	0.86	0.82	180	0.86	0.89	0.85
$(PAA_{60})_{21}$	60	35 (1.11)	54 (1.13)	61 (1.06)	–	–	–	–	64	0.94	0.84	0.95
$(PAA_{100})_{21}$	97	40 (1.03)	–	104 (1.02)	120 (1.13)	0.81	–	0.87	118	0.82	–	0.88
$(PAA_{125})_{21}$	125	53 (1.03)	122 (1.12)	133 (1.03)	150 (1.26)	0.83	0.81	0.89	120	1.04	1.02	1.11

[a] Expected degree of polymerization from monomer to initiation site ratio and monomer conversion.
[b] $DP_{n,arm} = DP_{n,star}$ divided by the number of initiation sites per initiator molecule.
[c] Efficiency of initiation sites, f_i, determined as $f_i = DP_{n,expected}/DP_{n,arm,experimental}$.
[d] $f_{i,Univ.cal}$ determined as $f_i = DP_{n,PtBA\text{-}star}/DP_{n,arm,experimental}$.
[e] $f_{i,MALDI}$ determined as $f_i = DP_{n,PMA\text{-}star}/DP_{n,arm,experimental}$.

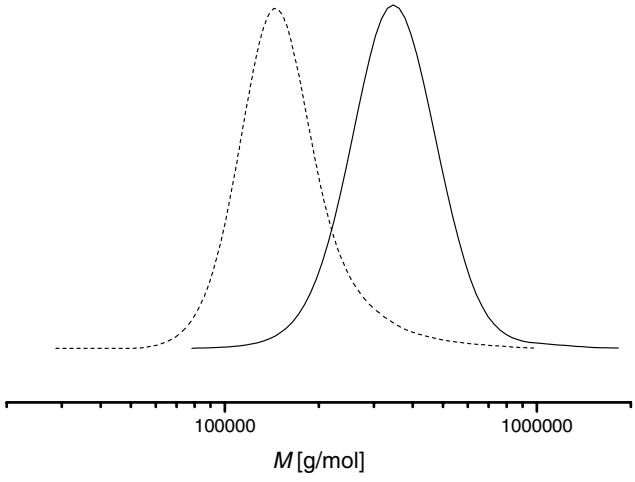

Figure 3. Molecular weight distributions of $(PtBA_{60})_{21}$ (- - -) and $(PtBA_{125})_{21}$ (—) determined by THF-GPC with viscosity detection (RI-traces).

tert-butyl groups were hydrolysed under these conditions (Figure 4). MALDI-TOF MS of pure PAA was not successful. According to the controlled character of ATRP, every polymer chain should have one initiation site moiety, as chain transfer to solvent or monomer and termination by recombination can be neglected, with respect to our GPC analysis. Additionally the length of the arms is still in the range in which end-group analysis is feasible. Therefore the DP_n of the PAA arms was determined by ^{1}H NMR analysis,

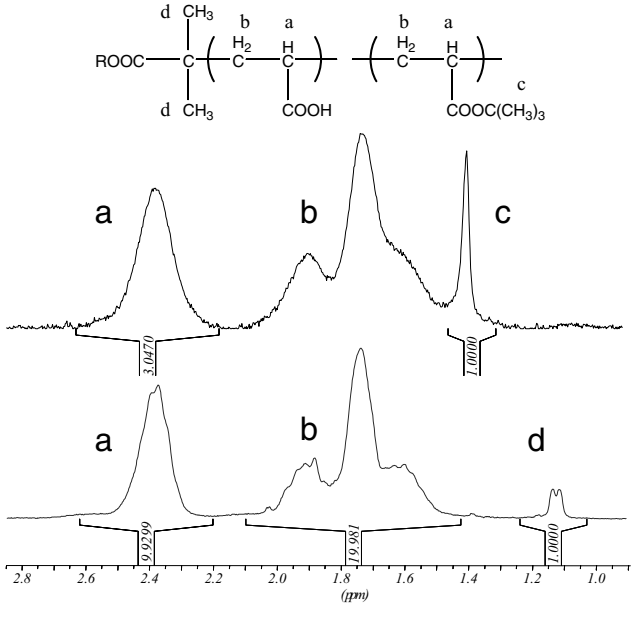

Figure 4. ^{1}H NMR spectra of $(PAA_{60})_{21}$ in D_2O after dialysis (top); the peak at 1.4 ppm originates from 4% residual *tert*-butyl groups. Bottom: linear PAA_{60} obtained from alkaline cleavage of arms; the pseudo-doublet at 1.1 ppm stems from the two methyl groups of the isobutyric acid initiator fragment.

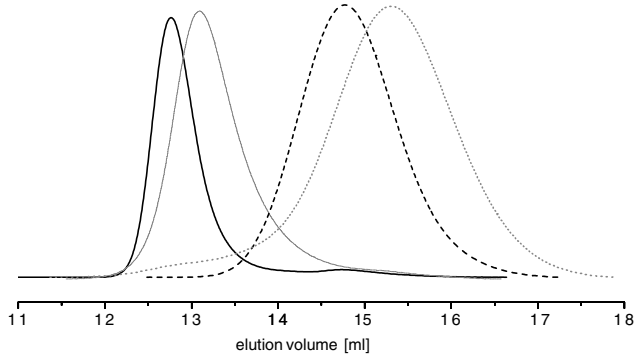

Figure 5. Aqueous GPC elution curves of $(PAA_{125})_{21}$ (—), $(PAA_{60})_{21}$ (·–·–·) and of the cleaved-off arms PAA_{125} (- - -) and PAA_{60} (···).

comparing the integrals I_{endgroup} over the methyl signals of the isobutyric acid end-group ($\delta = 1.1$ ppm) with those I_{methine} of the methine protons on the polymer backbone ($\delta = 2.4$ ppm) by Equation (2):

$$DP_n = 6 \cdot I_{\text{methine}} / I_{\text{endgroup}} \quad (2)$$

Some PAA stars were stored as rubidium salts (70% neutralization) at $pH \sim 7$ in aqueous solution at 5 °C for six months. Their SEC elution curves (in phosphate-buffered water) completely coincide with those obtained before, indicating that the stars are stable at neutral conditions in aqueous solution.

Since it is difficult to obtain absolute molecular weights in aqueous GPC, methylation was performed on the PAA stars and their cleaved-off arms. The ^{1}H and ^{13}C NMR spectra (Figure 6) of the methylated PAA show additional signals at 3.3 ppm, and 4.1 ppm for the ^{1}H NMR spectroscopy and 52.1 ppm and 58.9 ppm for the ^{13}C NMR spectroscopy. These additional signals may originate from methylene insertion into the C–O ester bond (similar to the generation of α-chloroketones from alkanoyl chlorides).[47,48] The only indication of the ketone carbonyl in the ^{13}C NMR spectrum was seen in the small peak at 174.8 ppm, which is shifted considerably upfield, compared to typical ^{13}C ketone signals (190–220 ppm). Additionally, we always find a triplet or pseudo-triplet at 3.4 ppm, which could not be assigned without doubt. According to the NMR spectroscopy, conversion to methyl ester was always at around 80%, and the majority of the residual acid groups were transformed to ketones. Thus almost no free acid groups remained and hydrophobization was complete. This was confirmed by the disappearance of the H–O vibration in the IR spectra. The $DP_{n,\text{arm}}$, determined by ^{1}H NMR end-group analysis of the PMA arms was in good agreement with those obtained from the PAA arms.

The star shaped poly(methyl acrylate)s (PMA) and their linear equivalents gave MALDI-TOF MS spectra in the expected molecular mass range (see experimental section,

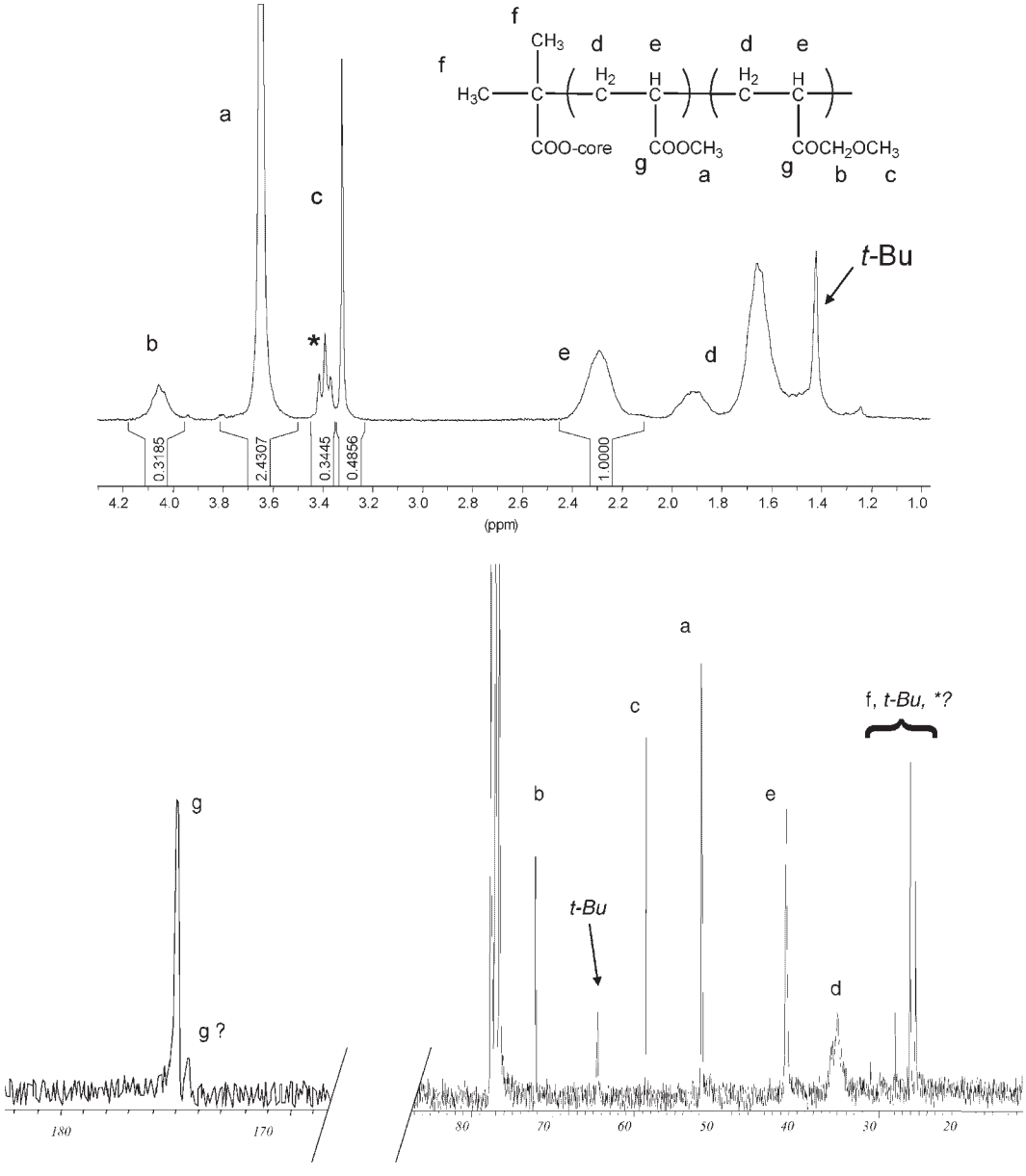

Figure 6. ^{1}H-NMR (top) and ^{13}C-NMR (bottom) spectrum of a methylated PAA star in $CDCl_3$; the most probable assignment of structures to the signals is shown; the asterisk designates a signal which cannot be completely assigned.

Figure 7). They often appear noisy, however, due to limited statistics (PMA did not fly deliberately). For results, see Table 2 and for details of the evaluation see the experimental section.

Table 2 sums up the molecular weight characterization for all polymers synthesized. The arm lengths of the PtBA and PMA stars are calculated by dividing the DP_n of the stars by the number of respective initiation sites per oligo-initiator. As expected, the arm lengths determined from GPC of the PtBA stars, using calibration with linear polystyrene standards, are lower than those obtained by the viscosity detector and using universal calibration. This is due to the well-known fact that stars have a lower hydrodynamic volume than linear polymers of the same molecular weight. Thus the former values have to be taken as apparent ones only.

Using the reasonable assumption that at least one initiating site in each oligo-initiator was active in initiating the polymer chains, the determined molecular weights of the PtBA or PMA stars should be equal to those expected from the monomer/initiation site ratio and monomer conversion. The deviations between these data are typically in the range of $\pm 5\%$, and, in some cases, up to $\pm 12\%$, showing the possible errors of the determination of monomer conversion by GPC of PTBA with universal calibration, and MALDI-TOF MS of PMA.

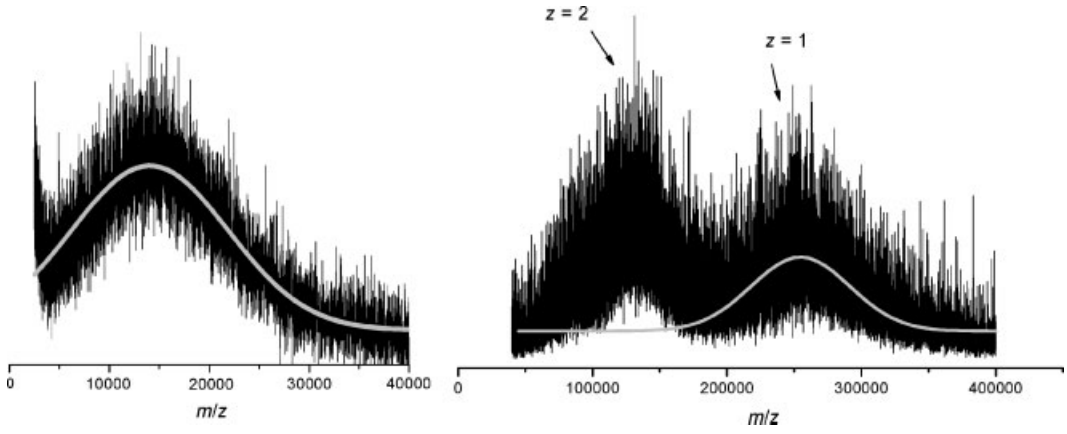

Figure 7. MALDI-TOF spectra of $(PMA_{125})_{21}$ (right) and of its linear arm, PMA_{125}, (left) with Gaussian fits of the species of interest.

If all of the initiating sites in an oligo-initiator are not active, this will result in a star with a smaller number of arms (and arm number distribution), where each arm is longer than expected. This cannot be detected by analyzing the molecular weight of the star: we have to determine the molecular weight of the arms separately. This is why we cleaved the arms by alkaline hydrolysis and analyzed them using different methods. The initiation site efficiency can then be determined by comparing the arm's molecular weight with that calculated from conversion or from the star molecular weight.

Table 2 shows that the initiation site efficiencies, $f_i = DP_{n,\mathrm{theo,arm}}/DP_{n,\mathrm{exp,arm}}$, differ between those determined by MALDI-TOF MS of PMA arms and those from NMR spectroscopy of PAA arms. Whereas the average initiator functionality is 0.97, as determined by NMR spectroscopy, it is only 0.84 as determined by MALDI-TOF. Since we already determined the expected arm lengths by NMR spectroscopy we trust the NMR results more, for the experimental determination. Taking into account that the error in the overall functionality was between 5 and 12% and that some initiation efficiencies are apparently larger than one, we conclude that the initiation site efficiency is close to unity, i.e. $\geq$95%. At present we can only speculate on the reasons, why the chain lengths of the PMA arms determined by MALDI-TOF MS are higher (on average by approximately 15%) than the ones determined by NMR spectroscopy of the PAA arms.

Having shown that we have obtained well defined star-shaped poly(acrylic acid), we now want to present some preliminary investigations of their properties.

Potentiometric Titration

We performed potentiometric titrations of our stars, as well as of linear PAA obtained by alkaline cleavage of $(PAA_{100})_{21}$. In all cases, the PAA was purified before titration, either by ultra-filtration or dialysis.

The pH dependence on the degree of neutralization, $\alpha = [Na^+]/[COOH]_0$, where $[COOH]_0$ is the total concentration of carboxyl and carboxylate groups and $[Na^+]$ assigns the amount of added NaOH, is presented in Figure 8.

As seen in Figure 8 the shape of the titration curves is as expected for linear PAA[18,23,30] and does not change significantly with increasing arm number or length. However, with increasing arm number (at constant arm length), the titration curves shift to higher pH values and thus to higher apparent values of pK_a, which is taken as the pH at 50% neutralization (see Table 3). This is in qualitative agreement with theory.[24] It is due to the higher osmotic pressure inside the stars, caused by counterion confinement (see next section). This leads to a partial reversal of the acid-base reaction, that is to say, the formation of uncharged –COOH groups within the polyelectrolyte star. As a consequence of this process, the pH value will increase outside. This effect is believed to be more pronounced for higher arm numbers, and for higher degrees of neutralization, as the osmotic pressure inside the star increases with segment density and ionization degree (which, in good approximation, is equal to α).

These shifts in the titration curve are not just a consequence of increasing the overall molar mass but rather a consequence of changing the degree of branching. The titration curve for linear PAA shows almost no dependence on the molecular weight, in the range 2×10^3 to 8×10^5 g · mol^{-1}.[49] We could show by use of stars with the same arm number but different arm lengths (see inset in Figure 8), that with increasing arm length the apparent pK_a values even decrease. Increasing $DP_{n,\mathrm{arm}}$ decreases the mean segment density within the star and less NaOH is expelled due to the lowered osmotic pressure.

The results are listed in Table 3.

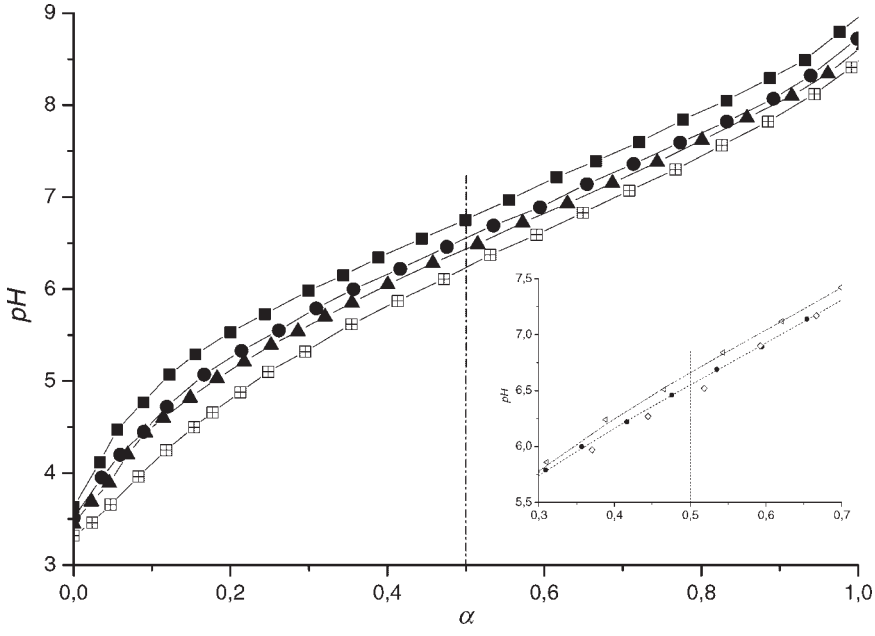

Figure 8. Potentiometric titration curves for stars $(PAA_{100})_{21}$ (■), $(PAA_{100})_8$ (●), $(PAA_{100})_5$ (▲), and linear PAA_{100} (⊞). Inset: cut-out of titration of $(PAA_{75})_8$ (△), $(PAA_{160})_8$ (◇), and $(PAA_{100})_8$ (●).

Osmometry – Determination of the Osmotic Coefficient

The osmotic coefficient describes the amount of released (cationic) counterions in case of (anionic) polyions. We calculated the osmotic coefficient, ϕ, by use of Equation (3), where Π_m denotes the measured osmotic pressure and Π_{cal} is the calculated osmotic pressure according to van't Hoff's law.

$$\phi = \frac{\Pi_m}{\Pi_{cal}} = \frac{\Pi_m(\alpha \cdot M_{ANa} + (1-\alpha) \cdot M_{AA})}{cRT\alpha} \qquad (3)$$

The degree of neutralization, α, is again the number of sodium ions per polymer repeat unit, the molar mass of which is given by the average of the sodium acrylate (M_{ANa}) and acrylic acid molar masses (M_{AA}), weighted by α. α is obtained by comparison of the measured pH value of a reference solution with the titration curves in Figure 8. The reference solution should have similar concentration as used for the potentiometric titrations. c is the mass concentration of the polyelectrolyte.

Sodium salts (NaPA) of PAA stars were prepared by use of NaOH. These salts were purified by dialysis to remove low molecular impurities like $NaHCO_3$. After two weeks, the pH changed significantly when dialysing 7 $g \cdot L^{-1}$ of $(PAA)_x$ sodium salt solution, adjusted to a pH of 7 to 8 with NaOH. Resulting in $pH \sim 5.5$, the dissociation degree, α, decreased from 0.6 to 0.25 (see Figure 8). The same principle, discussed in context with the titration curves, holds true, and NaOH, obtained by protolysis of the salt of the weak polyacid, is expelled out of the dialysis tube due to the high osmotic pressure inside. Carbon dioxide, which can hardly be excluded, has an accelerating effect. This process only takes place for dialysis and not for ultrafiltration, as only dialysis provides equilibrium between both sides of the membrane. We therefore only investigated star-shaped sodium salts of poly(acrylic acid) with a low ionization degree $\alpha \cong 0.25$ at different concentrations. The dialysed samples of partially neutralized $(PAA_{100})_8$ and $(PAA_{100})_{21}$ show a constant osmotic pressure during osmometry in the time frame of the experiments (30 min).

The dilute regime heading towards semi-dilute concentrations is depicted in Figure 9. The overlap concentration of $(PAA_{100})_{21}$ is approximately 4 $g \cdot L^{-1}$, whereas $(PAA_{100})_8$ overlaps at approximately 1.5 $g \cdot L^{-1}$. The overlap concentrations were calculated as the concentrations at

Table 3. Apparent pK_a values of different PAA stars[a].

	PAA_{100}	$(PAA_{90})_5$	$(PAA_{75})_8$	$(PAA_{100})_8$	$(PAA_{160})_8$	$(PAA_{100})_{21}$
$pK_{a,app}$	6.22	6.42	6.65	6.55	6.48	6.74

[a] The error in $pK_{a,app}$ is taken as ±0.05, the error in the pH determination.

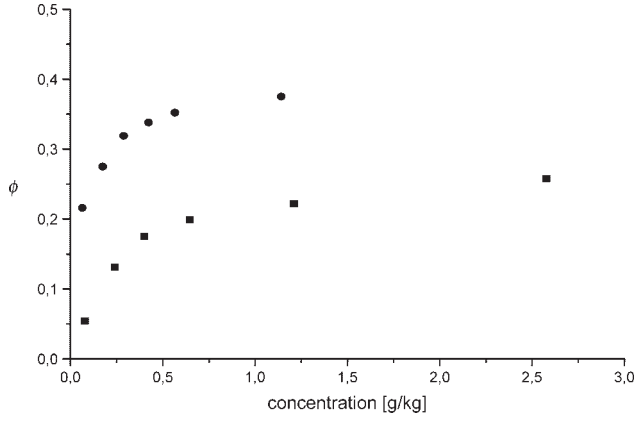

Figure 9. Osmotic coefficients ϕ of $(PAA_{100})_{21}$ (■, $\alpha = 0.24$) and $(PAA_{100})_8$ (●, $\alpha = 0.25$) in dependence of concentration.

which the stars occupy the total available solution volume, when they are regarded as spheres, with a single arm's contour length as the radius (assuming full extension of arms; 250 pm per monomer unit). This means these values are lower limits, although stacking factors were not taken into account.

In this context we should be aware that Manning's parameter[5] $\xi_M = l_B/b$, where b is the average charge to charge distance along the chain and l_B is the Bjerrum length, is smaller than unity for $\alpha \sim 0.25$. Thus, Manning condensation of counterions along the backbone of the polyelectrolyte chains does not take place ($\xi_M < 1$). However, we do measure an osmotic coefficient <0.4 which is due to the confinement of counterions within the star.

We find that the osmotic coefficient, ϕ, decreases with increasing arm number (or segment density), which is in qualitative agreement with prediction of theory.[22] For low arm numbers the stars' polyelectrolyte effect, related to the confinement of counterions, is not very pronounced, as the literature typically reports osmotic coefficients around 0.2 for fully charged linear PAA (NaPA)[16,20,50] and around 0.4 for partially charged PAA ($\alpha \sim 0.25$ (Figure 4 in ref.[16])). At sufficiently high arm number, we do observe the intermediate behavior between the linear and the brush-like polyelectrolytes. The theory assumes an equidistant charge distribution along the arm's backbone.[22] This may not hold true for our system at low ionization degrees (here: $\alpha \sim 0.25$) and charge annealing can take place, leading to a higher charge density on the periphery of the star. This is believed to promote counterion release.

In contrast to previous theoretical work applied to polyelectrolyte brushes,[51] the osmotic coefficient increases at higher concentrations. This was also observed by Deserno et al.[52] for rigid rod-like polyelectrolytes. They took into account the influence of small excess salt concentrations (impurities), which leads to a lowering of the osmotic coefficient.[16,53] With the help of Monte-Carlo simulations, Belloni et al. found similar concentration trends for star-like micelles.[54]

A more systematic theoretical and experimental study for the determination of counterion confinement in star-shaped polyelectrolytes will be given in a future publication.

Conclusion

Well defined poly(acrylic acid) stars could be prepared by ATRP of *tert*-butylacrylate with consecutive elimination of isobutylene. Different characterization methods showed that both arm lengths could be adjusted and verified, with the arm number close to the theoretical value. The titration curves of the PAA stars are shifted towards higher pH for increasing arm number. This was explained by the increasing segment density and the increasing osmotic pressure inside the stars. For higher arm numbers, the osmotic coefficient was considerably lower, as predicted by theory.

Acknowledgements: We appreciate the help of *Manuela Fink*, *Günther Jutz*, *Denise Danz*, *Xavier André*, *Sharmila Muthukrishnan*, *Youyong Xu* and *S. Wunder* during MALDI-TOF MS and GPC measurements, respectively. We thank *Arben Jusufi* for helpful discussions. The financial support by the *Deutsche Forschungsgemeinschaft* within SFB 481 is acknowledged.

[1] I. U. Rau, M. Rehahn, *Acta Polym.* **1994**, *45*, 3.
[2] C. Holm, M. Rehahn, W. Oppermann, M. Ballauff, *Adv. Polym. Sci.* **2004**, *166*, 1.
[3] R. Fuoss, A. Katchalsky, S. Lifson, *Proc. Natl. Acad. Sci. USA* **1951**, *37*, 579.
[4] N. Imai, F. Osawa, *Busseiron Kenkyu* **1953**, *46*, 14.
[5] G. S. Manning, *J. Chem. Phys.* **1969**, *51*, 924.
[6] H. Mori, D. Chan Seng, H. Lechner, M. Zhang, A. H. E. Müller, *Macromolecules* **2002**, *35*, 9270.
[7] H. Mori, A. Walther, X. André, M. G. Lanzendörfer, A. H. E. Müller, *Macromolecules* **2004**, *37*, 2054.
[8] J. Bohrisch, C. D. Eisenbach, W. Jaeger, H. Mori, A. H. E. Müller, M. Rehahn, C. Schaller, S. Traser, P. Wittmeyer, *Adv. Polym. Sci.* **2004**, *165*, 1.
[9] J. Rühe, M. Ballauff, M. Biesalski, P. Dziezok, F. Gröhn, D. Johannsmann, N. Houbenov, N. Hugenberg, R. Konradi, S. Minko, M. Motornov, R. R. Netz, M. Schmidt, C. Seidel, M. Stamm, T. Stephan, D. Usov, H. Zhang, *Adv. in Polym. Sci.* **2004**, *165*, 79.
[10] M. Biesalski, J. Rühe, *Macromolecules* **1999**, *32*, 2309.
[11] M. Ballauff, in: *Polymer Brushes*, R. C. Advincula, Ed., Wiley-VCH Verlag GmbH & Co. KGaA, Weinheim, Germany 2004, p. 231.
[12] G. Cheng, A. Böker, M. Zhang, G. Krausch, A. H. E. Müller, *Macromolecules* **2001**, *34*, 6883.
[13] M. Zhang, T. Breiner, H. Mori, A. H. E. Müller, *Polymer* **2003**, *44*, 1449.
[14] X. Guo, M. Ballauff, *Phys. Rev. E: Stat., Nonlinear, & Soft Matter Phys.* **2001**, *64*, 051406/1.

[15] Y. Mei, M. Ballauff, *Eur. Phys. J. E: Soft Matter* **2005**, *16*, 341.
[16] A. Katchalsky, *Pure Appl. Chem.* **1971**, *26*, 327.
[17] B. Das, X. Guo, M. Ballauff, *Prog. Colloid Polym. Sci.* **2002**, *121*, 34.
[18] W. Kern, *Z. Physik. Chem.* **1938**, *A181*, 249.
[19] N. Ise, T. Okubo, *J. Phys. Chem.* **1967**, *71*, 1287.
[20] R. Kakehashi, H. Yamazoe, H. Maeda, *Colloid Polym. Sci.* **1998**, *276*, 28.
[21] B. Zhang, D. Yu, H.-L. Liu, Y. Hu, *Polymer* **2002**, *43*, 2975.
[22] A. Jusufi, C. N. Likos, H. Löwen, *J. Chem. Phys.* **2002**, *116*, 11011.
[23] J. Klein Wolterink, F. A. M. Leermakers, G. J. Fleer, L. K. Koopal, E. B. Zhulina, O. V. Borisov, *Macromolecules* **1999**, *32*, 2365.
[24] J. K. Wolterink, J. van Male, M. A. C. Stuart, L. K. Koopal, E. B. Zhulina, O. V. Borisov, *Macromolecules* **2002**, *35*, 9176.
[25] O. V. Borisov, E. B. Zhulina, *Journal de Physique II* **1997**, *7*, 449.
[26] O. V. Borisov, E. B. Zhulina, *Eur. Phys. J. B: Condens. Matter Phys.* **1998**, *4*, 205.
[27] C. N. Likos, N. Hoffmann, A. Jusufi, H. Löwen, *J. Phys: Condens. Matter* **2003**, *15*, 233.
[28] N. Hoffmann, C. N. Likos, H. Löwen, *J. Chem. Phys.* **2004**, *121*.
[29] T. Furukawa, K. Ishizu, *Macromolecules* **2005**, *38*, 2911.
[30] A. Katchalsky, J. Gillis, *Recueil des Travaux Chimiques des Pays-Bas et de la Belgique* **1949**, *68*, 879.
[31] M. Borkovec, G. J. M. Koper, *Ber. Bunsen-Gesellschaft* **1996**, *100*, 764.
[32] J. de Groot, G. J. M. Koper, M. Borkovec, J. de Bleijser, *Macromolecules* **1998**, *31*, 4182.
[33] M. Borkovec, G. J. M. Koper, *Macromolecules* **1997**, *30*, 2151.
[34] J. W. Mays, *Polym. Commun.* **1990**, *31*, 170.
[35] M. Heinrich, M. Rawiso, J. G. Zilliox, P. Lesieur, J. P. Simon, *Eur. Phys. J. E: Soft Matter* **2001**, *4*, 131.
[36] D. Held, A. H. E. Müller, *Macromol. Symp.* **2000**, *157*, 225.
[37] M. Pitsikalis, S. Sioula, S. Pispas, N. Hadjichristidis, D. C. Cook, J. Li, J. W. Mays, *J. Polym. Sci., Part A: Polym. Chem.* **1999**, *37*, 4337.
[38] C. Mengel, W. H. Meyer, G. Wegner, *Macromol. Chem. Phys.* **2001**, *202*, 1138.
[39] M. Schnitter, J. Engelking, A. Heise, R. D. Miller, H. Menzel, *Macromol. Chem. Phys.* **2000**, *201*, 1504.
[40] D. Moinard, D. Taton, Y. Gnanou, C. Rochas, R. Borsali, *Macromol. Chem. Phys.* **2003**, *204*, 89.
[41] K. Ohno, D. M. Haddleton, D. Kukulj, B. Wong, *Polym. Prepr. (Am. Chem. Soc., Div. Polym. Chem.)* **2000**, *41*, 478.
[42] M. H. Stenzel-Rosenbaum, T. P. Davis, V. Chen, A. G. Fane, *Macromolecules* **2001**, *34*, 5433.
[43] D. M. Haddleton, R. Edmonds, A. M. Heming, E. J. Kelly, D. Kukulj, *New J. Chem.* **1999**, *23*, 477.
[44] R. Edmonds, S. A. F. Bon, D. M. Haddleton, *Polym. Prepr. (Am. Chem. Soc., Div. Polym. Chem.)* **2000**, *41*, 444.
[45] L. Couvreur, C. Lefay, J. Belleney, B. Charleux, O. Guerret, S. Magnet, *Macromolecules* **2003**, *36*, 8260.
[46] H. Benoit, Z. Grubisic, P. Rempp, D. Decker, J. G. Zilliox, *Macromolecules* **1966**, *63*, 1507.
[47] D. A. Clibbens, M. Nierenstein, *J. Chem. Soc., Abstr.* **1915**, *107*, 1491.
[48] R. E. Van Atta, H. D. Zook, P. J. Elving, *J. Am. Chem. Soc.* **1954**, *76*, 1185.
[49] S. Kawaguchi, T. Takahashi, H. Tajima, Y. Hirose, K. Ito, *Polymer J. (Tokyo)* **1996**, *28*, 735.
[50] N. Ise, *Fortschr. Hochpolymer.-Forsch.* **1971**, *7*, 536.
[51] A. Jusufi, C. N. Likos, M. Ballauff, *Colloid Polym. Sci.* **2004**, *282*, 910.
[52] M. Deserno, C. Holm, J. Blaul, M. Ballauff, M. Rehahn, *Eur. Phys. J. E: Soft Matter* **2001**, *5*, 97.
[53] E. Raspaud, M. da Conceicao, F. Livolant, *Phys. Rev. Lett.* **2000**, *84*, 2533.
[54] L. Belloni, M. Delsanti, P. Fontaine, F. Muller, P. Guenoun, J. W. Mays, P. Boesecke, M. Alba, *J. Chem. Phys.* **2003**, *119*, 7560.

